Toward an Allosteric Metallated Container

ARTICLE *in* EUROPEAN JOURNAL OF INORGANIC CHEMISTRY · JANUARY 2009

Impact Factor: 2.94 · DOI: 10.1002/ejic.200800659

4 AUTHORS, INCLUDING:

Morsy Abu-Youssef
Alexandria University
90 PUBLICATIONS **1,685** CITATIONS

DOI: 10.1002/ejic.200800659

Toward an Allosteric Metallated Container

Helga Szelke,[a] Hubert Wadepohl,[a] Morsy Abu-Youssef,[a,b] and Roland Krämer*[a]

Keywords: Allosterism / Supramolecular chemistry / Cage compounds / Iron / Ruthenium

Polytopic ligands L^1 and L^2 in which three 2,2′-bipyridine units are linked to a central tris(pyrid-2-yl)amine (L^1) or tris-(pyrid-2-yl)methanol (L^2) moiety by alkyl spacers were prepared by multistep organic syntheses. The parent tris(pyrid-2-yl)-type ligands were shown to be modest-to-good chelators for Zn^{2+} and Cu^{2+} ions in solution, and bi- and tridentate N-coordination was confirmed by crystal structures of Cu^{II} and Ru^{II} complexes, respectively. Fe^{II} and Ru^{II} smoothly form stable, cage-like 1:1 complexes with L^1 and L^2, in which the metal ion is coordinated to the tris(bpy) site of the ligands. The vacant tris(pyrid-2-yl) site of these complexes is, however, a poor donor site for Zn^{2+} and Cu^{2+} ions. In addition, Fe^{II} modulates the coordination behaviour of the tris(pyrid-2-yl) site toward Zn^{2+}: Whereas tris(5-methylpyrid-2-yl)amine forms a 2:1 complex with Zn^{2+} in CH_2Cl_2, $[Fe(L^1)]^{2+}$ forms a 1:1 Zn complex. Spectrophotometric titrations suggest that $[Fe(L^2)]^{2+}$ forms a polynuclear Zn^{2+} complex in CH_2Cl_2, possibly involving bridging coordination of the alcohol OH group, which contrasts the smooth formation of a 2:1 complex of the parent tris(pyrid-2-yl)-type ligand with Zn. Fe^{II} might therefore be considered as an allosteric effector, which modulates the metal binding properties of the second tris(pyrid-2-yl) site of L^1 and L^2. Contrary to expectation, Zn^{2+} and Cu^{2+} appear to associate weakly with donor atoms directed toward the exterior of the cage-like complexes $[Fe(L^n)]^{2+}$ and $[Ru(L^1)]^{2+}$, rather than locating in the interior of the container by tripodal coordination to the tris(pyrid-2-yl) site.

Introduction

Metal-ion cofactors of metalloproteins are often located in discrete cavities that support selective and effective substrate binding and/or protection of reactive metal-bound species. Chemists were inspired early to prepare low-molecular weight coordination compounds that effectively mimic the shielding of such reactive metal sites.[1] The design of such compounds has meanwhile developed into an important research line in bioinorganic and supramolecular chemistry, including "metallated containers"[2] and calixarene-based "funnel complexes".[3] In this context, complexes of tripodal ligands that mimic the tris(imidazole) donor sites in a number of zinc and copper proteins have attracted considerable attention;[4] open cavities around the metal site are generated by attachment of bulky substituents to the ligating groups. Substrate selectivity and shielding might be further optimized by complete encapsulation of the metal ion within a cage-like ligand framework without hindering access of the substrate to free metal sites, but synthesis of such compounds is expected to be more challenging and less versatile.

Here we suggest a supramolecular approach to the development of a cage-like compound for incorporation of both a reactive metal ion and a substrate (Scheme 1). A tripodal tris(pyrid-2-yl)amine or -methanol unit serves as an analogue of the biological tris(imidazole) metal-binding site. Substituents are appended at the 5-position (rather than the 6-position) of the pyridyl rings in order to avoid steric hindrance of substrate binding by the metal ion and guarantee adequate cavity size for incorporation of small-molecule substrates. Three bidentate 2,2-bipyridine units are linked to the tripodal moiety by alkyl spacers in a manner that ring closure and formation of a bicyclic cage is achieved by intramolecular, metal-assisted assembly (Scheme 1). This

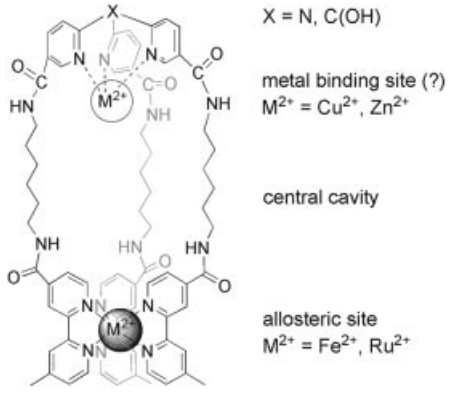

Scheme 1.

[a] Anorganisch-Chemisches Institut der Universiät Heidelberg, Im Neuenheimer Feld 270, 69120 Heidelberg, Germany
Fax: +49-6221-548599
E-mail: roland.kraemer@urz.uni-heidelberg.de
[b] On leave from Chemistry Department, Faculty of Science, Alexandria University, 21321 Alexandria, Egypt

strategy avoids potentially complicated covalent synthesis of a relatively large bicyclic structure. In addition, considering the polytopic ligand as a ditopic receptor, coordination of a metal ion to the tris(bpy) site is expected to modify the metal binding properties of the tris(pyrid-2-yl) site, as described for a variety of synthetic allosteric receptors[5] for metal ions. Here we will describe the synthesis of the polytopic ligands, their interaction with transition-metal ions and an allosteric relation between the two metal binding sites [tris(bpy) and tri(pyrid-2-yl)] of the ditopic receptors.

Results and Discussion

Ligand Synthesis

The synthetic route to polytopic ligands L^1 [tridentate site: tris(pyrid-2-yl)amine] and L^2 [tridentate site: tris(pyrid-2-yl)methanol] is summarized in Scheme 2. 2,2′-Bipyridine derivative **1** was synthesized by coupling the linker *N*-Boc-1,6-diaminohexane to 4′-methyl-2,2′-bipyridine-4-carboxylic acid[6] by using a standard amide coupling reaction, followed by removal of the Boc protecting group under acidic conditions. Tris(2-pyridyl)amine derivative **2** was prepared by the reaction of 2-amino-5-picoline and 2-bromo-5-methylpyridine over copper bronze. The methyl groups of **2** were oxidized to the corresponding tris(2-nicotinic acid)-amine (**3**) by using potassium permanganate as an oxidant. Finally, **3** was joined to three bipyridine units **1** by amide coupling to yield ligand L^1 (Scheme 2).

Tris(2-nicotinic acid)methanol (**5**) was synthesized by the oxidation of the methyl groups of tris[(5-methylpyrid-2-yl)]-methanol (**4**)[7] as described in the literature.[8] Three units of bipyridine derivative **1** were coupled to **5** as described for L^1 above to give ligand L^2 (Scheme 2). The latter was available in low quantity so that only selected experiments and analytics could be performed (Scheme 3).

Interaction of 2 and 4 with Zn^{2+} and Cu^{2+} in Solution

We characterized the coordination of Zn^{2+} and Cu^{2+} biometals to the simple tripodal ligands **2** and **4** in solution to achieve a better understanding of the interaction of these exchange-labile metal ions with the tris(pyrid-2-yl) site in more complex ligands L^1 and L^2.

Tris(pyrid-2-yl)amine was reported to form (depending on the ligand-to-metal ratio) a tetrahedral 1:1 complex with $ZnCl_2$ and an octahedral 2:1 complex with $Zn(O_2CCF_3)_2$ in the crystalline state.[9] In both complexes, tris(pyrid-2-yl)amine coordinates in a bidentate fashion, and planarity around the central N atom is retained. Bidentate coordination, although with fluctional behaviour, is retained in dichloromethane solution, as evidenced by NMR spectroscopy. Similarly, both 1:1 and 2:1 complexes with Cu^{II} have been reported, again with bidentate coordination of tris(pyrid-2-yl)amine. In contrast, in the presence of weakly coordinating perchlorate counterion, octahedral 2:1 complexes with exchange labile Co^{II} and Ni^{II} were reported in which tris(pyrid-2-yl)amine is tridentate.[10] The coordination mode of tris(pyrid-2-yl)amine appears to be controlled by specific preferences of the transition metal. Possibly, a loss of *N*-aryl resonance energy due to pyramidalization slightly disfavours a tripodal coordination. On the basis of ball-and-stick models and preliminary force field calculations, we speculated that preorganization of the pyridyl do-

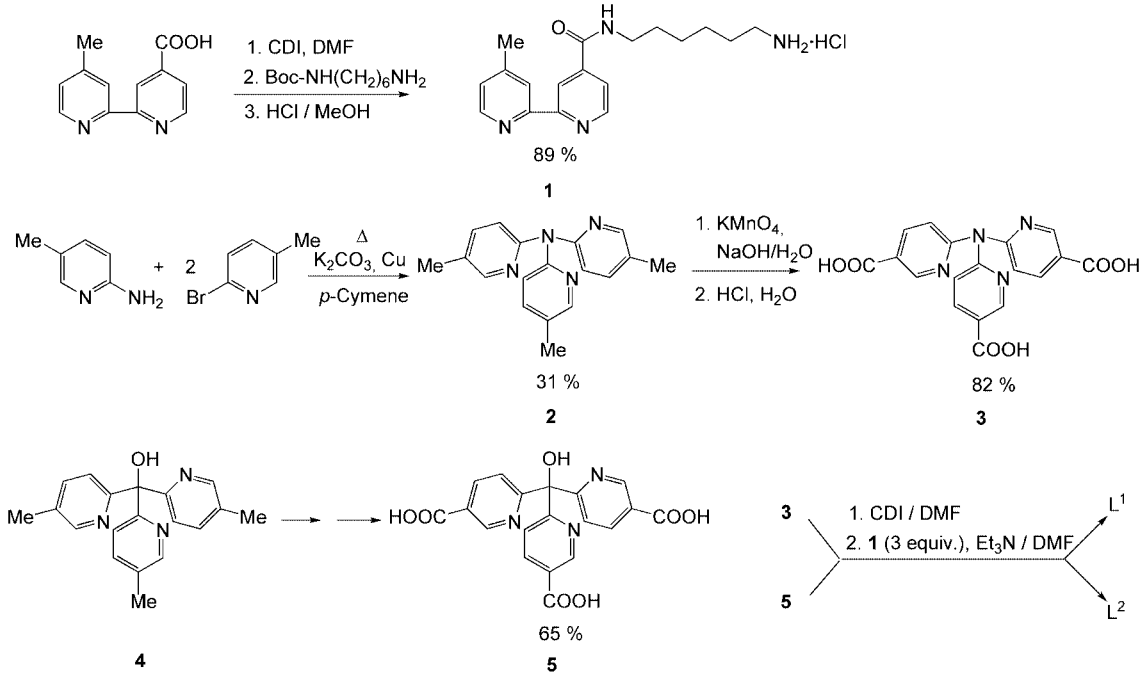

Scheme 2. Synthesis of L^1 and L^2.

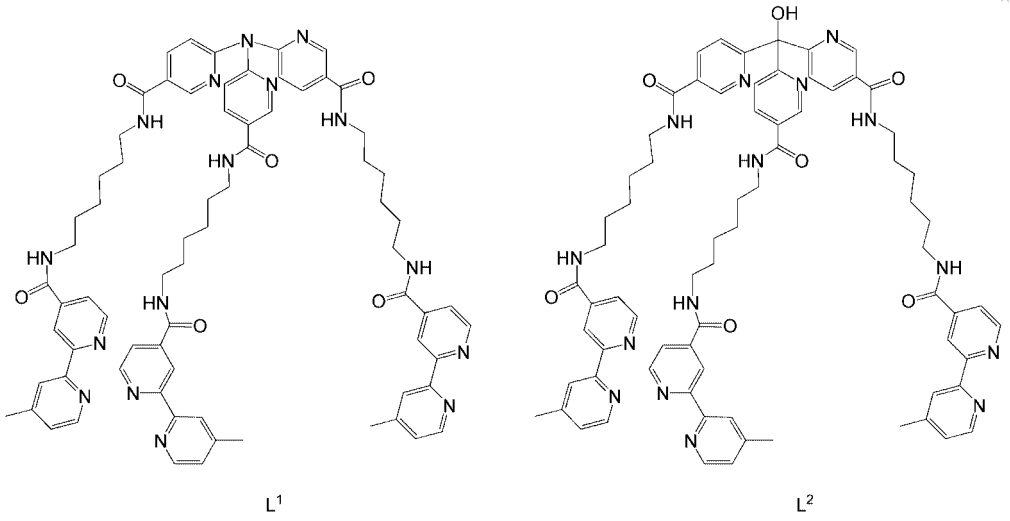

Scheme 3. Structure of polytopic ligands L^1 and L^2.

nors in the cage-like structure depicted in Scheme 1 would favour tripodal coordination of Zn and Cu. In addition, coordination of two cage-like moieties to one zinc or copper ion should be disfavoured.

Interaction of **2** with Zn is solvent and counterion dependent; in 50 μM solutions of **2** in water/methanol mixtures the UV/Vis spectra exhibit no changes upon addition of the Zn^{2+} salts, indicating no complexation. Smooth complexation of **2** by Zn is observed in the noncompetitive solvent CH_2Cl_2 in the presence of the weakly coordinated counterion ClO_4^-. Upon the addition of $Zn(ClO_4)_2$ (0–0.5 equiv.) to a (50 μM) solution of **2**, a significant and nearly linear decrease in the 272 and 302 nm absorbances of the ligand together with two isosbestic points at 260 and 326 nm is observed (Figure 1). This is compatible with the formation of a complex $[Zn(\mathbf{2})_2]^{2+}$. The minor changes observed in the UV spectrum upon addition of 0.5–1.0 equiv. of Zn^{2+} (enlarged absorbance diagram, Figure 1, right) might indicate conversion of the 2:1 into a 1:1 complex $[\{Zn(\mathbf{2})\}^{2+}]$. Formation of 2:1 and 1:1 complexes with Zn^{2+} in CD_2Cl_2, depending on the ligand-to-metal ratio, was also described of for tris(pyrid-2-yl)amine on the basis of NMR spectroscopic investigations.[9]

Cu^{2+} forms stronger complexes with **2** than Zn^{2+}, as indicated by the titration of **2** (1 mM) with $Cu(NO_3)_2$ solution in competitive solvent water/methanol (3:1) containing 10 mM MOPS buffer at pH 7.0 and 50 mM NaCl. A shoulder appears at about 410 nm together with a broad absorbance at 650 nm (Figure 2). The plot of the absorption intensity at 410 nm against the Cu^{2+} equivalents indicates about 90% complex formation at 1.0 equiv. and saturation at about 2 equiv. Formation of a green 1:1 Cu^{2+} complex with bidentate coordination of tris(5-methylpyrid-2-yl)amine was confirmed by X-ray structural analysis (see below) of the crystalline precipitate formed when the solution was treated with $NaClO_4$ and allowed to stand for several days at ambient temperature. In the noncompetitive solvent CH_2Cl_2, the

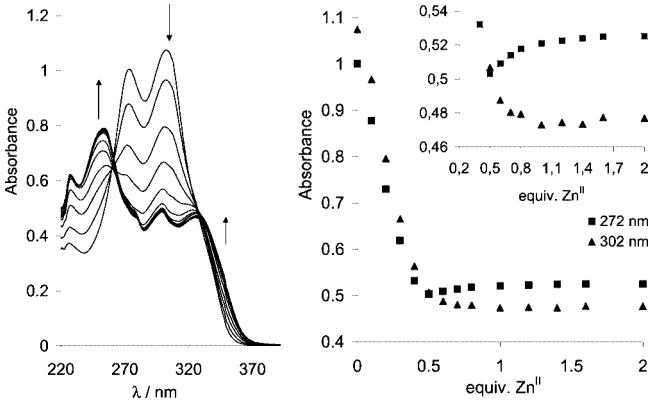

Figure 1. Spectrophotometric titration of **2** (50 μM in CH_2Cl_2) with $Zn(ClO_4)_2$ in 0.1 equiv. steps. Inset: decrease in the absorbance at 272 nm (■) and at 302 nm (▲).

titration of **2** with $Cu(ClO_4)_2$ compares well with the Zn titration, suggesting stepwise formation of 2:1 and 1:1 complexes.

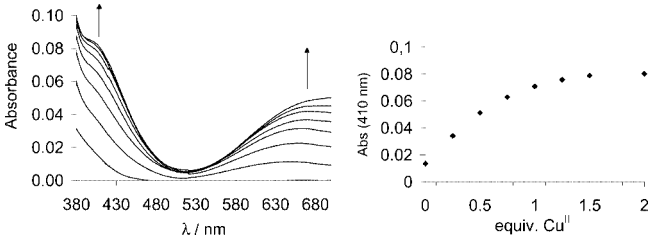

Figure 2. Spectrophotometric titration of **2** (1 mM in H_2O/MeOH, 3:1; pH 7.0; 10 mM MOPS buffer; 50 mM NaCl) with $Cu(NO_3)$. Left: increase in the absorbance at 410 nm.

Tris(pyrid-2-yl)methanol (**4**) is expected to form more stable tripodal transition-metal complexes due to better preorganization of the pyridyl groups linked to the central sp^3 carbon atom. In contrast, the coordination mode is am-

biguous due to potential participation of the (deprotonated) OH group in metal binding. Compound **4** in mM concentration was shown by NMR spectroscopy to preferably form a 2:1 Zn^{2+} complex in aqueous solution and a mixture of 1:1 and 2:1 complexes in acetonitrile solution, both with tripodal N,N,N-coordination.[8,11] Tris(6-methoxypyrid-2-yl)methanol, a ligand related to **4**, was shown to form a distorted octahedral 2:1 complex with Cu^{2+} (crystal structure), again with tridentate N,N,N-coordination of both ligands (Figure 3).[12]

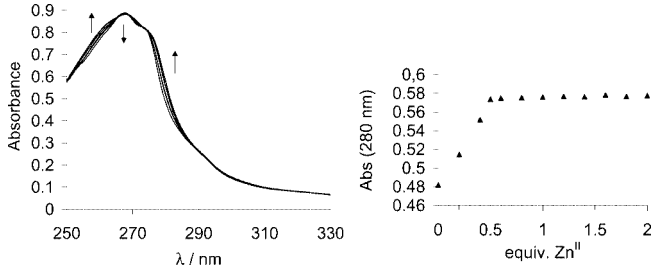

Figure 3. Spectrophotometric titration of **4** (50 μM in H_2O/MeOH, 1:1; pH 7.0; 10 mM MOPS buffer; 50 mM NaCl) with $ZnSO_4$. Left: increase in the absorbance at 280 nm.

Spectrophotometric titration of **4** (50 μM) with $ZnSO_4$ in water/methanol (1:1) was followed by relatively small absorbance changes in the UV region of the spectrum and confirms smooth formation of a complex $[Zn(\mathbf{4})_2]^{2+}$ by linear absorbance increase at 280 nm for 0–0.5 equiv. of Zn^{2+}. No further changes are observed at >0.5 equiv. of Zn^{2+}, but conversion into a 1:1 complex with a large excess of Zn^{2+} is not ruled out.

When **4** is titrated with $CuSO_4$ under the same conditions, a significant increase in the absorbance at 330 nm is observed, together with development of a weak absorbance in the visible spectrum at about 600 nm (Figure 4). The 330 nm absorbance diagram suggests stepwise formation of complexes $[Cu(\mathbf{4})_2]^{2+}$ at 0.5 equiv. of Cu^{2+} and $[Cu(\mathbf{4})]^{2+}$ at 1 equiv. of Cu^{2+}, which might have slightly different absorbance maxima in the optical spectrum.

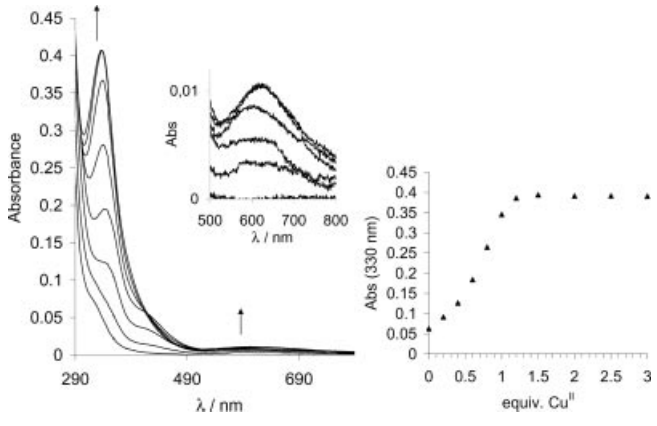

Figure 4. Spectrophotometric titration of **4** (50 μM in H_2O/MeOH, 1:1; pH 7.0; 10 mM MOPS buffer; 50 mM NaCl) with $CuSO_4$. Inset: increase in the absorbance at 610 nm. Left: increase in the absorbance at 280 nm.

X-ray Crystallography of 2 and Its Metal Complexes

Structure of Tris(3-methyl-pyrid-2-yl)amine

The X-ray crystal structure of tris(pyrid-2-yl)amine was reported only recently,[9] and **2** has, to the best of our knowledge, not yet been crystallographically characterized.

As in tris(pyrid-2-yl)amine, the central nitrogen atom N1 in **2** is nearly coplanar with the three adjacent carbon atoms; the deviation from the $(C)_3$ plane is only 0.041(1) Å. The dihedral angles between the pyridyl rings and the $(C)_3$ plane were found to be 23.0, 40.2 and 40.9° (Figure 5).

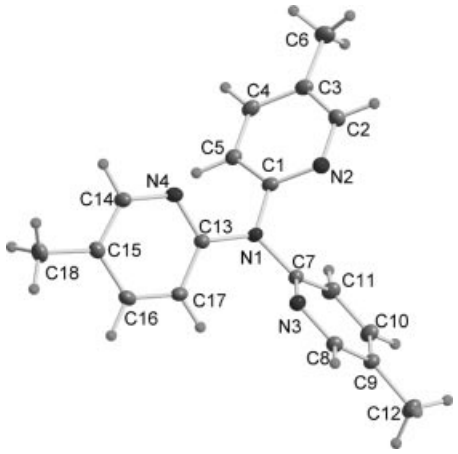

Figure 5. ORTEP diagram showing the structure of **2** with 50% thermal ellipsoids and the atom-labelling scheme.

Structure of [(2)Cu(H$_2$O)$_2$(NO$_3$)](ClO$_4$)·2H$_2$O

The X-ray structure of the complex cation of **2**, [(**2**)$Cu(H_2O)_2(NO_3)](ClO_4)\cdot 2H_2O$, which was obtained by mixing solutions of **2** and $Cu(NO_3)_2$ with the addition of $NaClO_4$, is shown in Figure 6. The Cu^{2+} ion displays a distorted octahedral environment (CuN_2O_4). Compound **2** acts as an N,N′-bidentate chelating ligand with Cu–N bond lengths of 1.973(3) and 1.981(3) Å and an N–Cu–N angle of 88.7(1)°. Planarity of the central N atom in complex **2**·Cu is retained, where the deviation of N1 from the $(C)_3$ plane [0.014(4) Å] was found to be smaller than that in the free ligand. The dihedral angle between the uncoordinated pyridyl ring and the $(C)_3$ plane was found to be 76.9°,

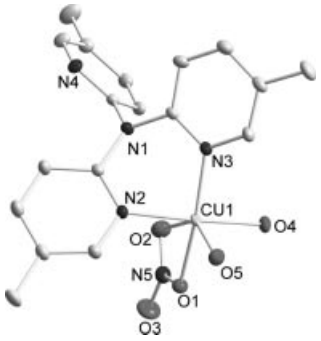

Figure 6. ORTEP diagram showing the structure of [(**2**)$Cu(H_2O)_2(NO_3)]^+$ complex cation with 50% thermal ellipsoids and the atom-labelling scheme. Hydrogen atoms are omitted for clarity.

whereas the coordinated pyridine rings keep nearly the same 40.9 and 44.4°. The Cu–O(water) bond lengths are 1.944(2) and 2.168(3) Å, whereas the Cu–O(nitrate) distances are 2.034(2) and 2.656(3) Å. Bond angles around the central Cu ion range from 81.5(1) to 98.8(1)°, except the O–Cu–O angle of the chelating nitrate, which was found to be 53.24(9)°. Bidentate coordination by the tris(pyrid-2-yl)-amine moiety is also found in other crystallographically characterized Cu^{II} complexes: [L = tris(pyrid-2-yl)amine]; $[Cu_4L_4\text{-}\mu(OH)_4(F_3CSO_3)_2]\cdot F_3CSO_3\cdot OC(CH_3)_2$,[13] $[CuL_2(NCCH_3)_2]\cdot F_3CSO_3$,[14] $[CuL_2(NO_3)_2]$[15] and $[CuL_2(ClO_4)_2]$.[16]

Structure of [(2)$_2$Ru](PF$_6$)$_2$

Orange crystals of the complex $[Ru(\mathbf{2})_2](PF_6)_2$ (Figure 7) were obtained by reaction of **2** with $RuCl_2(dmso)_4$, followed by precipitation of the complex cation with PF_6^- and recrystallization from methanol. The complex cation is octahedral with a crystallographic centre of symmetry. The Ru–N(py) bond lengths range from 2.064(2) to 2.073(2) Å and the N–Ru–N bond angles range from 86.20(7) to 93.80(7)°, indicating a nearly perfect octahedral coordination of Ru^{II} by two tridentate moieties of **2**. Very similar bonding parameters around Ru^{II} have been reported for the following complexes [L = tris(pyrid-2-yl)amine]: $[RuL_2]S_2O_6\cdot H_2O$ and $[RuL_2]Cl_2\cdot H_2O$.[17,18]

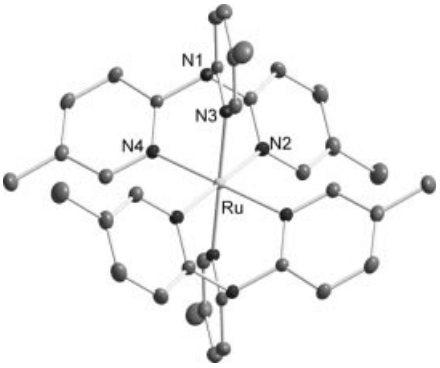

Figure 7. ORTEP diagram showing the structure of $Ru[(\mathbf{2})_2]^{2+}$ complex cation with 50% thermal ellipsoids and the atom-labelling scheme. Hydrogen atoms are omitted for clarity.

Interaction of Polytopic Ligands L^1 and L^2 with Metal Ions

Binding of Fe^{II} to L^1 and L^2

The complexation behaviour of the polytopic ligands L^1 and L^2 with Fe^{2+} (offered as BF_4^- salt) in CH_2Cl_2 at 25 °C was monitored by spectrophotometric titration. Smooth formation of a 1:1 complex is indicated by two isosbestic points at 269 and 290 nm (Figure 8).

Absorbance at selected wavelengths 360 and 537 nm increases linearly upon addition of 0–1 equiv. of Fe^{2+}. The absorption band around 537 nm is characteristic for the MLCT of the Fe[tris(2,2′-bipyridine)]$^{2+}$ octahedral complex,[19] which forms in a cooperative manner with a very high stability constant $\log(\beta_3) = 21$ in water. It is therefore

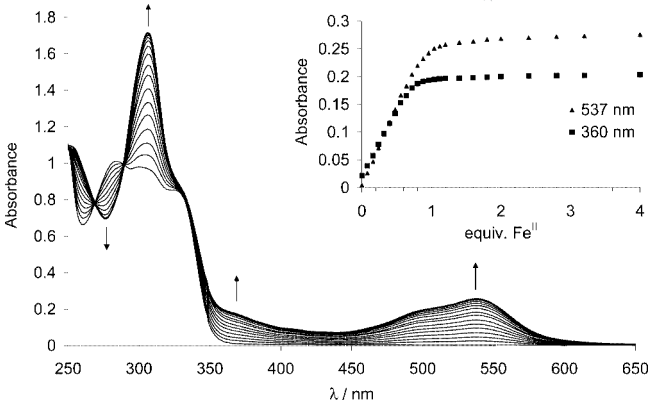

Figure 8. Spectrophotometric titration of **2** (25 μM in CH_2Cl_2) with $Fe(BF_4)_2$. Inset: increase in the absorbance at 360 nm (■) and at 537 nm (▲).

very likely that Fe^{2+} forms an octahedral complex with the tris(bpy) site of L^1. The red 1:1 complex $[Fe(L^1)](ClO_4)_2$ could be isolated and characterized by MS (ESI) and elemental analysis. Thus, Fe^{2+} assembles the tricyclic cage-like structure as expected. The same conclusion can be drawn when L^1 is titrated with Fe^{2+} in more competitive solvents (methanol, dmso/water mixtures). Smooth binding of Fe^{2+} to a tris(bpy) site was described previously for related tribrachial ligands with three 2,2-bipyridine moieties linked by aza–polyether, aza–thioether or hydroxamic acid containing chains. In these compounds, the Fe^{2+} ion organizes as cryptand-like structures and allosterically controls the binding of alkali-metal ions or transition-metal ions, respectively.[20] Upon addition of >1 equiv. of Fe to L^1, no further spectral changes are observed between 250 and 650 nm, indicating that even in the noncompetitive solvent CH_2Cl_2, additional Fe^{2+} does not interact with the vacant tris(pyrid-2-yl)amine site of the complex.

Very similar spectrophotometric changes are observed when L^2 is titrated with 0–1 equiv. of $Fe(BF_4)_2$ under the same conditions (Figure 9), although the 1:1 complex could not be isolated in pure form. Interestingly and in contrast to the behaviour of L^1, a further linear increase in the 360 nm absorbance of L^2 is observed upon addition of 1–4 equiv. of Fe and levels off at >4 equiv., whereas the 537 nm band remains unchanged. An increase in the 360 nm band suggests interaction of the free pyridyl groups with Fe, but the L^1:Fe stoichiometry is not compatible with a binding of just a second Fe^{2+} ion to the tris(pyrid-2yl) site in the interior of the cage. Rather, the OH group in L^2 might act as a bridging ligand {as observed for the Cu^{2+} ions in the related complex $[Cu_3(Br)(L)_3](PF_6)_2$,[21] where L = tris(6-methyl-2-pyridyl)methanol}, for up to three Fe^{II} ions with additional coordination by one pyridyl group each and located at the exterior of the cage.

^{1}H NMR spectra of $[Fe(L^1)](BF_4)_2$ were taken in CD_3OD solutions containing 20% $[D_6]$dmso. At room temperature, the spectrum of aromatic protons displays broad featureless signals, which overlap a set of sharp signals. When the sample is heated to 60 °C, the intensity of the

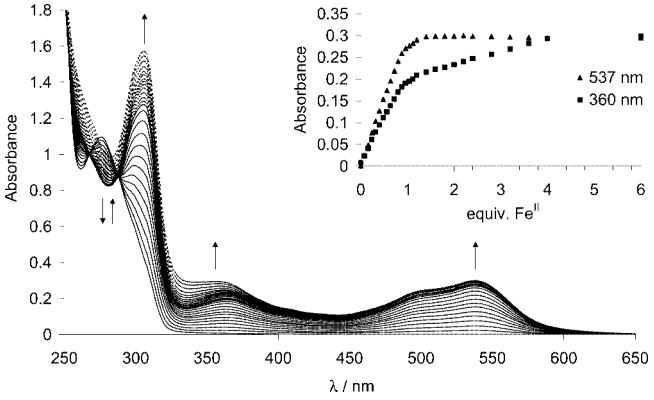

Figure 9. Spectrophotometric titration of **4** (25 μM in CH_2Cl_2) with $Fe(BF_4)_2$ in 0–1 equiv. steps (solid lines) and 1–6 equiv. steps (dashed lines). Inset: increase in the absorbance at 360 nm (■) and at 537 nm (▲).

sharp signals increases and that of the broad signals decreases. The final spectrum remains unchanged after cooling to room temperature, even after prolonged standing. A reasonable interpretation of this observation is the formation of two diastereomers due to chirality of both the $Fe(bpy)_3$ site and the NPy_3 "propeller", which give rise to different sets of NMR signals (broad and sharp, respectively). When the complex is prepared at room temperature, diastereomer formation is under kinetic control, yielding a mixture of isomers. Upon heating to 60 °C, the configuration of the $Fe(bpy)_3$ moiety becomes labile, leading to equilibration and enrichment of the thermodynamically favoured second isomer with sharp NMR signals.

Binding of Ru^{II} to L^1

L^1 reacted with 1 equiv. of $RuCl_3$ at elevated temperature to give the red complex $[Ru(L^1)]Cl_2$. Its composition was confirmed by HRMS (ESI) and elemental analysis. Selective binding of Ru^{II} to the tris(bpy) site is supported by a characteristic MLCT absorbance at λ_{max} = 460 nm, together with a corresponding fluorescence at λ_{em} = 630 nm (Figure 10) as observed for the complex $[Ru(bpy)_3]^{2+}$.[22] In contrast, the Ru^{II} complex of **2**, $[Ru(\mathbf{2})_2]^{2+}$, is yellow with an absorbance maximum at 396 nm. Whereas the Fe^{2+} ion in $Fe(L^1)$ can be removed by prolonged treatment with a large excess of EDTA or by exchange with an excess amount of Cu^{2+} ions, $[Ru(L^1)]Cl_2$ is not affected by these reagents and, as expected, displays very high kinetic stability.

The ^1H NMR spectra of $[Ru(L^1)]Cl_2$ in CD_3OD look similar to those of the corresponding Fe^{II} complex at room temperature. However, the spectrum remains unchanged after heating to 60 °C. This is consistent with the kinetic inertness of the $Ru(bpy)_3$ unit, which prevents equilibration of the diastereomer mixture.

Interaction of Fe^{II}(L^n) and Ru^{II}(L^1) with Zn^{2+} and Cu^{2+}

When the 1:1 iron(II) complexes of L^1 and L^2 are exposed to $CuSO_4$ in aqueous systems, the 537 nm band characteristic of the $Fe^{II}(bpy)_3$ unit slowly decreases, indicating replacement of Fe^{2+} by Cu^{2+} at the bpy site of L^n. In contrast, fluorescence titration of the stable $Ru^{II}(L^1)$ complex with Cu^{2+} in aqueous systems indicates an interaction by significant 630 nm fluorescence quenching at 0–1 equiv. of Cu. This is, however, not accompanied by the characteristic absorbance changes in the UV region of the spectrum, which were seen in the titration of **2** with Cu. We therefore suggest association of Cu^{2+} at the exterior of the cage, at a site other than bis- or tris(pyrid-2-yl).

When solutions of $Fe^{II}(L^1)$, $Fe^{II}(L^2)$ and $Ru^{II}(L^1)$ were titrated with $ZnSO_4$ in aqueous solvent mixtures, no spectral changes were observed between 250 and 650 nm. As observed for **2**, Zn^{2+} does not interact with the tris(pyrid-2-yl) site of $Fe^{II}(L^1)$ in competitive solvents. In the noncompetitive solvent CH_2Cl_2, however, a titration of $[Fe(L^1)](BF_4)_2$ with $Zn(ClO_4)_2$ reveals similar changes in the UV absorbance as observed for **2** (Figure 11), but the 330 nm absorbance diagram indicates formation of a 1:1 complex (whereas a 2:1 ligand/metal complex was formed with **2**, see Figure 1). This observation alone does not allow the conclusion of Zn binding in the interior of the container as depicted in Scheme 1, although a reason for the lack of 2:1 complex formation, which might form by interaction of Zn^{2+} with external binding sites of *two* $Fe^{II}(L^1)$ moieties, is

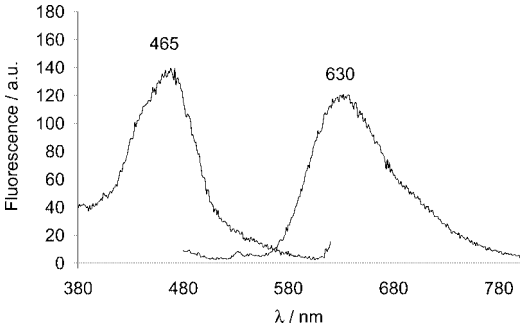

Figure 10. $Ru(bpy)_3$ centred fluorescence emission spectrum (630 nm) of $[Ru(L^1)]Cl_2$ (5 μM in EtOH/H_2O, 1:1; pH 7.0; 10 mM MOPS). Absorbance spectrum (λ_{max} = 465 nm) is included.

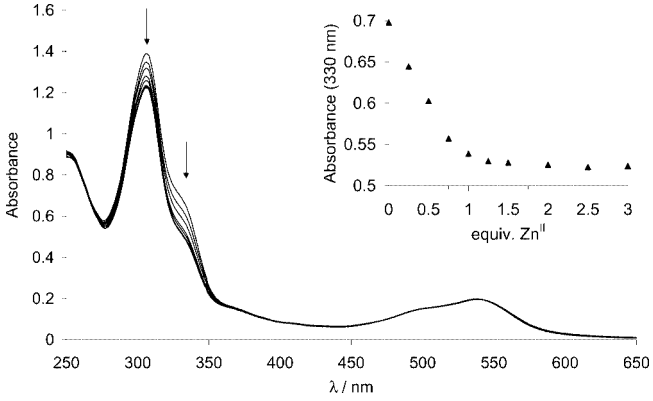

Figure 11. Spectrophotometric titration of $[Fe(L^1)](BF_4)_2$ (20 μM in CH_2Cl_2) with $Zn(ClO_4)_2$. Inset: increase in the absorbance at 330 nm.

not obvious. Unfortunately, the NMR spectra of $Fe^{II}(L^1)$ in the presence or absence of Zn^{2+} display broad signals only and are not helpful for determination of Zn binding mode.

The same experimental conditions were kept to study the interaction of $[Fe(L^2)](BF_4)_2$ in CH_2Cl_2 with $Zn(ClO_4)_2$ (data not shown). We noticed a small increase in the absorption intensity at 305 nm and a decrease at 285 nm, with an isosbestic point at 296 nm, indicating interaction of Zn^{2+} with the pyridyl units of $[Fe(L^2)](BF_4)_2$. However, as in the titration of $[Fe(L^2)](BF_4)_2$ with excess Fe^{2+}, spectral changes do not level off after 1 equiv. of Zn^{2+}, again indicating formation of polynuclear Zn^{II} complexes at exterior binding sites.

Conclusions

We prepared tribrachial ligands L^1 and L^2, which offer two distinct sites for metal-ion coordination: a tridentate tris(pyrid-2-yl) site and a tris(bidentate) 2,2′-bipyridyl site. These ligands form stable, cage-like 1:1 complexes with Fe^{II} and Ru^{II}, which coordinate to the tris(bpy) site with high selectivity. Whereas the parent tris(pyrid-2-yl)-type ligands are moderate-to-good binders of exchange-labile metal ions Zn^{2+} and Cu^{2+} in solution, the tris(pyrid-2-yl) site within the cage-type complexes is a poor ligand, indicating negative allostery in transition-metal binding of L^1 and L^2. Spectrophotometric titrations suggest weak association of Zn^{II} and Cu^{II} with donor groups orientated to the exterior of the cage rather than incorporation of these metal ions in the interior of the container by tridentate coordination to the tris(pyrid-2-yl) site. The reasons for this unexpected behaviour might include stabilization of the "empty" container by intramolecular hydrophobic interactions, intramolecular electrostatic repulsion of the two metal ions and enforced desolvation of the metal ion within the container. Redesign of the polytopic ligand is currently in progress. In addition, we are trying to attach exchange inert transition-metal ions to the tris(pyrid-2-yl) site of L^n, after selective protection of bpy moieties.

Experimental Section

General: Commercially available chemicals were purchased from Sigma–Aldrich (Germany) and used without purification. 4′-Methyl[2,2′]bipyridine-4-carboxylic acid,[6] tris[2-(5-methylpyridyl)]-methanol (**4**),[7] tris(2-nicotinic acid)methanol (**5**)[8] and $RuCl_2(dmso)_4$[23] were synthesized as described in the literature. NMR spectra were obtained with Bruker Avance 200 and 400 MHz spectrometers, chemical shifts are given in ppm relative to Me_4Si, coupling constants are given in Hz. ESI mass spectra were measured with a Q-TOF Ultima ESI-MS instrument (Waters-Micromass). Elemental analyses were performed by Microanalytisches Laboratorium des Organisch-Chemischen Instituts der Universität Heidelberg.

***N*-(Aminohexyl)-4′-methyl-2,2′-bipyridine-4-carboxamide·HCl (1):** A solution of 4′-methyl-2,2′-bipyridine-4-carboxylic acid (1.0 g, 4.7 mmol) and 1,1′-carbonyldiimidazole (CDI; 0.83 g, 4.7 mmol) in dry DMF (15 mL) was stirred at 60 °C under an atmosphere of nitrogen for 30 min. Then, a solution of *N*-Boc-1,6-diaminohexane (1.0 g, 4.7 mmol) in dry DMF (10 mL) was added dropwise and stirring was continued at 60 °C under an atmosphere of nitrogen for 16 h. Solvent was removed under reduced pressure, and the residue was taken up in chloroform (100 mL). This solution was filtered to remove residues of unreacted carboxylic acid, and the filtrate was extracted with saturated NH_4Cl (50 mL) and brine (50 mL). The organic phase was dried with $MgSO_4$, filtered and the solvent was removed under reduced pressure to afford the Boc-protected amide (1.59 g, 83%) as a white solid. ^1H NMR (200 MHz, $CDCl_3$): δ = 1.34–1.53 (m, 6 H), 1.40 (s, 9 H), 1.59–1.69 (m, 2 H), 2.42 (s, 6 H), 3.11 (q, J = 7.2 Hz, 2 H), 3.44 (q, J = 6.4 Hz, 2 H), 4.57 [br. s, 1 H, NHC(O)], 6.72 [br. s, 1 H, NHC(O)], 7.17 (d, J = 5.0 Hz, 1 H), 7.78 (dd, J = 5.0 Hz, J = 1.6 Hz, 1 H), 8.26 (s, 1 H), 8.53 (d, J = 5.0 Hz, 1 H), 8.61 (s, 1 H), 8.78 (d, J = 5.0 Hz, 1 H) ppm. MS (ESI+): m/z = 413.2 $[M + H]^+$. The Boc protecting group was removed by dissolving the protected amide (1.59 g, 3.9 mmol) in methanol (30 mL) and adding HCl/H_2O (1:1, 30 mL). After stirring at room temperature for 16 h, the solvent was removed under reduced pressure. The residue was taken up in methanol, and the product was precipitated with ether. The precipitate was filtered, washed with diethyl ether and vacuum dried to give a white solid (1.20 g, 89%). ^1H NMR (200 MHz, [D$_6$]dmso): δ = 1.32–1.41 (m, 4 H), 1.48–1.62 (m, 4 H), 2.57 (s, 3 H), 2.75 (q, J = 6.4 Hz, 2 H), 3.32 (q, J = 6.0 Hz, 2 H), 7.65 (d, J = 5.2 Hz, 1 H), 7.99 (d, J = 5.0 Hz, 1 H), 8.05 (br. s, 3 H), 8.65 (s, 1 H), 8.69 (d, J = 5.4 Hz, 1 H), 8.91 (d, J = 5.0 Hz, 1 H), 8.96 (s, 1 H), 9.23 [br. t, 1 H, NHC(O)] ppm. HRMS (ESI+): calcd. for $C_{18}H_{25}N_4O$ $[M + H]^+$ 313.2028; found 313.2018.

Tris[2-(5-methylpyridyl)]amine (2): 2-Bromo-5-methylpyridine (6.52 g, 38 mmol), 5-methylpyridin-2-amine (2.05 g, 19 mmol), potassium carbonate (4.36 g, 44 mmol), potassium iodide (trace) and potassium bromide (trace) were heated at reflux (60 h) with continuous stirring over copper (0.95 g, 15 mmol) in *p*-cymene (30 mL). The product mixture was filtered hot and washed with ethanol, and the solvent was removed under reduced pressure. The product was purified by column chromatography (silica gel, 3% methanol in dichloromethane) and recrystallized from acetone/hexane to afford a yellow crystalline product (1.67 g, 30%). X-ray quality crystals were grown by slow crystallization at room temperature from ethanol. ^1H NMR (200 MHz, $CDCl_3$): δ = 2.27 (s, 9 H), 6.95 (d, J = 8.2 Hz, 3 H), 7.42 (dd, J = 8.2 Hz, J = 2.2 Hz, 3 H), 8.18 (d, J = 1.6 Hz, 3 H) ppm. HRMS (ESI+): calcd. for $C_{18}H_{19}N_4$ $[M + H]^+$ 291.1610; found 291.1590. UV/Vis (MeOH): λ_{max} (ε, $M^{-1}cm^{-1}$) = 270 (18730), 303 (21010) nm; λ_{em} = 400 nm.

Tris(2-nicotinic acid)amine (3): Amine **2** (1.14 g, 3.9 mmol), $KMnO_4$ (5.12 g, 32.4 mmol) and NaOH (1.41 g, 35.3 mmol) were added to distilled water (150 mL). The reaction mixture was stirred at 60 °C for 4 h. To this mixture a second portion of $KMnO_4$ (4.23 g, 26.8 mmol) was added and stirring was continued at 60 °C for 16 h. The reaction was quenched with methanol, and the brown precipitate (MnO_2) was filtered off and washed with water. The combined aqueous phase was acidified with HCl/H_2O (1:1) to pH 2.5 and was cooled to 5 °C. The resulting white precipitate was filtered off, washed with water and dried in vacuo to give triacid **3** (1.2 g, 82%) as a white powder. ^1H NMR (200 MHz, MeOD): δ = 7.27 (d, J = 8.6 Hz, 3 H), 8.34 (dd, J = 8.5 Hz, J = 2.2 Hz, 3 H), 8.92 (d, J = 2.2 Hz, 3 H) ppm. HRMS (ESI+): calcd. for $C_{18}H_{13}N_4O_6$ $[M + H]^+$ 381.0835; found 381.0845.

L^1: A solution of triacid **3** (0.25 g, 0.66 mmol) and 1,1′-carbonyldiimidazole (CDI; 0.39 g, 2.17 mmol) in dry DMF (20 mL) was stirred at 60 °C under an atmosphere of nitrogen for 30 min. Then, a solution of aminobipyridine **1** (0.76 g, 2.17 mmol) and Et_3N (0.4 mL, 2.89 mmol) in dry DMF (20 mL) was added dropwise and stirring was continued at 60 °C under an atmosphere of nitrogen for 16 h. The solvent was removed under reduced pressure, and the residue was taken up in methanol/chloroform (1:2, 15 mL). An insoluble white powder was filtered off, and the remaining solution was concentrated in vacuo. The residue was purified by column chromatography (neutral alumina, 5% methanol in chloroform) followed by precipitation from methanol/chloroform (1:2) with ether to give the product (0.19 g, 23%) as a white powder. ^{1}H NMR (200 MHz, $CDCl_3$): δ = 1.28–1.36 (m, 12 H), 1.46–1.58 (m, 12 H), 2.38 (s, 9 H), 3.26–3.37 (m, 12 H), 6.94 (d, J = 8.4 Hz, 3 H), 7.11 (d, J = 4.6 Hz, 3 H), 7.66 [br. t, 3 H, NHC(O)], 7.68 (d, J = 4.2 Hz, 3 H), 8.00 (dd, J = 8.8 Hz, J = 1.2 Hz, 3 H), 8.14 (s, 3 H), 8.39 (d, J = 5.0 Hz, 3 H), 8.53 (s, 3 H), 8.65 (s, 3 H), 8.67 (d, J = 5.4 Hz, 3 H) ppm. HRMS (ESI+): calcd. for $C_{72}H_{80}N_{16}O_6$ $[M + H]^+$ 1264.6447; found 1264.6438. UV/Vis (CH_2Cl_2): λ_{max} (ε, $M^{-1}cm^{-1}$) = 284 (50530), 300 (49000), 324 (sh.) nm; λ_{em} = 400 nm.

L^2: A solution of triacid **5** (0.1 g, 0.25 mmol) and 1,1′-carbonyldiimidazole (CDI; 0.12 g, 0.75 mmol) in dry DMF (10 mL) was stirred at 60 °C under an atmosphere of nitrogen for 30 min. Then, a solution of aminobipyridine **1** (0.25 g, 0.72 mmol) and Et_3N (0.16 mL, 0.84 mmol) in dry DMF (15 mL) was added dropwise and stirring was continued at 60 °C under an atmosphere of nitrogen for 16 h. The solvent was removed under reduced pressure, and the residue was purified by column chromatography (silica gel, 5% methanol in chloroform) followed by precipitation from methanol/chloroform (1:2) with ether to give the product (93 mg, 30%) as an off-white powder. ^{1}H NMR (400 MHz, $CDCl_3$): δ = 1.18–1.23 (m, 12 H), 1.38–1.46 (m, 12 H), 2.34 (s, 9 H), 3.24–3.29 (m, 12 H), 7.04 (d, J = 4.8 Hz, 3 H), 7.48–7.57 (m, 6 H), 7.62 (dd, J = 4.8 Hz, J = 1.6 Hz, 3 H), 7.72 [br. t, 3 H, NHC(O)], 7.98 (d, J = 8.8 Hz, 3 H), 8.12 (s, 3 H), 8.34 (d, J = 5.2 Hz, 3 H), 8.59 (s, 3 H), 8.61 (d, J = 4.8 Hz, 3 H), 8.83 (s, 3 H) ppm. HRMS (ESI+): calcd. for $C_{73}H_{81}N_{15}O_7$ $[M + H]^+$ 1279.6443; found 1279.6490. UV/Vis (CH_2Cl_2): λ_{max} (ε, $M^{-1}cm^{-1}$) = 275 (45570) nm; λ_{em} = 360 nm.

$[(2)Cu(NO_3)(H_2O)_2](ClO_4)\cdot 2H_2O$: To a solution of ligand **2** (67 mg, 0.23 mmol) dissolved in acetone (5 mL) was added a solution of $Cu(NO_3)_2$ in water (0.5 M, 0.46 mL), and the mixture was stirred at room temperature for 2 h. Then, a solution of $NaClO_4$ (28 mg, 0.23 mmol) in water (5 mL) was added, and the mixture was allowed to stand overnight. Dark-green crystals appeared that were filtered off, washed with diethyl ether and dried to afford the product (91 mg, 72%). MS (ESI+): m/z (%) = 415.0 (100) $[^{63}Cu(\mathbf{2})(NO_3)]^+$, 417.0 (65) $[^{65}Cu(\mathbf{2})(NO_3)]^+$, 452.0 (49) $[^{63}Cu(\mathbf{2})(NO_3)]^+$, 454.0 (32) $[^{65}Cu(\mathbf{2})(NO_3)]^+$. UV/Vis (MeOH/$H_2O$, 1:1): λ_{max} (ε, $M^{-1}cm^{-1}$) = 265 (22200), 300 (23900), 400 (80), 658 (52) nm.

$[Ru(2)_2](PF_4)_2$: A mixture of ligand **2** (25 mg, 0.087 mmol) and $RuCl_2(dmso)_4$ (20 mg, 0.041 mmol) was heated in ethylene glycol (10 mL) at 125 °C for 10 min under an atmosphere of nitrogen. After cooling down to room temperature, water (10 mL) was added, and the product was precipitated with saturated NH_4PF_6. The precipitate was filtered off, washed with water and vacuum dried to afford a yellow solid (25 mg, 61%). ^{1}H NMR (200 MHz, $CDCl_3$): δ = 2.08 (s, 18 H), 7.40 (br. s, 6 H), 8.00 (d, J = 1.4 Hz, 6 H), 8.04 (s, 16 H) ppm. MS (ESI+): m/z (%) = 341.4 (100) $[^{101}Ru(\mathbf{2})_2]^{2+}$, 827.1 (49) $[^{101}Ru(\mathbf{2})_2(PF_6)]^+$. UV/Vis (MeOH): λ_{max} (ε, $M^{-1}cm^{-1}$) = 252 (9650), 266 (sh.), 340 (4910), 396 (12070) nm.

$[Fe(L^1)](ClO_4)_2\cdot 4H_2O$: To a solution of ligand L^1 (20 mg, 0.016 mmol) dissolved in methanol/dichloromethane (1:1, 5 mL) was added a solution of $Fe(ClO_4)_2\cdot xH_2O$ in acetonitrile (0.1 M, 0.158 mL), and the mixture was stirred at room temperature for 2 h. A dark-red precipitate appeared upon standing that was filtered off, washed with dichloromethane and dried to afford a red solid (9.1 mg, 38%). HRMS (ESI+): calcd. for $C_{72}H_{78}N_{16}O_6Fe$ $[M + H]^+$ 1318.5640; found 1318.5616. $C_{72}H_{86}Cl_2N_{16}O_{18}Fe$ (1590.30): calcd. C 54.38, H 5.45, N 14.09; found C 54.59, H 5.53, N 14.25. UV/Vis (dmso/H_2O, 4:1): λ_{max} (ε, $M^{-1}cm^{-1}$) = 255 (53900), 308 (93700), 365 (sh.), 539 (10460) nm. ^{1}H NMR after heating to 60 °C, only signals of one diastereomer are given (400 MHz; [D$_6$]dmso/MeOD, 1:5): δ = 1.62–1.77 (m, 18 H), 1.79–1.88 (m, 6 H), 3.13–3.22 (m, 6 H), 3.42–3.51 (m, 9 H), 3.81–3.52 (m, 6 H), 7.13 (d, 3 H, J = 5.6 Hz), 7.16 (d, 3 H, J = 8.8 Hz), 7.38 (d, 3 H, J = 5.6 Hz), 7.58 (d, 3 H, J = 5.6 Hz), 7.92 (d, 3 H, J = 5.6 Hz), 8.20 (dd, 3 H, J = 8.8 Hz, J = 2.4 Hz), 8.48 (d, 3 H, J = 2.4 Hz), 8.69 (s, 3 H), 8.97 (s, 3 H).

$[Ru(L^1)]Cl_2\cdot 4H_2O$: A mixture of ligand L^1 (33 mg, 0.026 mmol) and $RuCl_3\cdot 3H_2O$ (6.5 mg, 0.025 mmol) was heated in ethanol (95%, 10 mL) at 78 °C for 16 h under an atmosphere of nitrogen. After cooling down to room temperature, the solvent was removed under reduced pressure and the residue was purified by column chromatography (neutral alumina, 1% AcOH, 15% methanol in chloroform) followed by precipitation from methanol with ether to afford an orange solid (18 mg, 44%). HRMS (ESI+): calcd. for $C_{72}H_{78}N_{16}O_6Ru$ $[M + H]^+$ 1364.5334; found 1364.5268. $C_{72}H_{86}Cl_2N_{16}O_{10}Ru$ (1507.53): C 57.36, H 5.75, N 14.87; found C 57.71, H 5.75, N 14.99. UV/Vis (MeOH/H_2O, 1:1): λ_{max} (ε, $M^{-1}cm^{-1}$) = 297 (84172), 325 (sh.), 459 (14180) nm; λ_{em} = 630 nm. ^{1}H NMR, only sharp signals of one diastereomer are given (400 MHz, MeOD): δ = 1.39–1.50 (m, 12 H), 1.61–1.73 (m, 12 H), 3.36 –3.48 (m, 12 H), 7.14 (d, 3 H, J = 8.4 Hz), 7.27 (d, 3 H, J = 4.4 Hz), 7.76 (d, 3 H, J = 4.4 Hz), 8.15 (d, 3 H, J = 8.4 Hz, J = 2.4 Hz), 8.18 (s, 3 H), 8.52 (d, 3 H, J = 4.8 Hz), 8.60 (s, 3 H), 8.74 (s, 3 H), 8.76 (d, 3 H, J = 5.0 Hz).

Spectrophotometric and Fluorescence Titrations: Fluorescence spectra were acquired with a Varian Cary Eclipse fluorescence spectrophotometer, UV/Vis experiments were performed with a Varian Cary 100 Bio UV/Vis spectrophotometer by using 1 cm optical path quartz or PMMA macrocuvettes with a sample volume of 2 mL.

X-ray Crystal Structure Determinations: Crystal data and details of the structure determinations are listed in Table 1. Intensity data were collected at low temperature with a Bruker AXS Smart 1000 CCD diffractometer and corrected for Lorentz, polarization and absorption effects (semiempirical, SADABS).[24] The structures were solved by the heavy atom method combined with structure expansion by direct methods applied to difference structure factors[25] or by conventional direct methods[26] (compound **2**) and refined by full-matrix least-squares methods based on F^2 against all reflections.[27] All non-hydrogen atoms were given anisotropic displacement parameters. For compound **2** the positions of most hydrogen atoms (except those of the methyl groups, which were treated as variable metric rigid groups) were taken from difference Fourier syntheses and refined. For all other structures, hydrogen atoms were input at calculated positions and refined with a riding model. In the structure of $[(\mathbf{2})Cu(H_2O)_2(NO_3)](ClO_4)\cdot 2H_2O$ the hydrogen atoms of the water molecules could not be unambiguously located. The perchlorate anion in this structure was found to be severely disordered; Cl–O and O···O distances were restrained to sensible values during refinement. CCDC-690411 (for **2**), -690412

Table 1. Details of the crystal structure determinations of compounds **2**, [(**2**)Cu(H_2O)$_2$(NO_3)](ClO_4)·2H_2O and [(**2**)$_2$Ru](PF_6)$_2$.

	2	[(**2**)Cu(H_2O)$_2$(NO_3)](ClO_4)·2H_2O	[(**2**)$_2$Ru](PF_6)$_2$
Formula	$C_{18}H_{18}N_4$	$C_{18}H_{26}ClCuN_5O_{11}$	$C_{36}H_{36}F_{12}N_8P_2Ru$
Crystal system	monoclinic	monoclinic	monoclinic
Space group	$P2_1/c$	$P2_1/c$	$P2_1/n$
a / Å	9.6470(6)	8.9902(5)	9.862(2)
b / Å	10.8779(7)	16.742(1)	11.342(2)
c / Å	15.2615(8)	16.293(1)	18.251(3)
β / °	110.420(3)	99.600(1)	104.539(3)
V / Å^3	1500.9(2)	2418.0(2)	1976.1(6)
Z	4	4	2
M_r	290.36	587.43	971.74
$d_{calcd.}$ / Mg m^{-3}	1.285	1.614	1.633
F(000)	616	1212	980
μ(Mo-K_α) / mm^{-1}	0.079	1.081	0.574
Max., min. transmission factors	0.9799, 0.9705	0.8246, 0.7230	0.7464, 0.6759
X-radiation, λ / Å	Mo-K_α, graphite monochromated, 0.71073		
Data collection temperature / K	100(2)	100(2)	100(2)
ϑ range / °	2.3 to 32.0	1.8 to 31.5	2.1 to 31.5
Index ranges (indep. set) h, k, l	–14 to 13, –15 to 0, –22 to 12	–13 to 13, 0 to 24, 0 to 23	–14 to 13, 0 to 16, 0 to 26
Reflections measured	14297	60716	49713
Unique [R_{int}]	5100 [0.0352]	7986 [0.0471]	6542 [0.0589]
Observed [$I \geq 2\sigma(I)$]	3842	6252	4908
Parameters refined	232	328	271
R indices [$F>4\sigma(F)$] $R(F)$, $wR(F^2)$	0.0537, 0.1425	0.0785, 0.2488	0.0370, 0.0809
R indices (all data) $R(F)$, $wR(F^2)$	0.0718, 0.1538	0.0933, 0.2652	0.0638, 0.0984
GooF on F^2	1.067	1.138	1.077
Largest residual peaks / e Å^{-3}	0.612, –0.236	3.682, –3.277	1.199, –0.514

{for [(**2**)Cu(H_2O)$_2$(NO_3)](ClO_4)·2H_2O} and -690413 {for [(**2**)$_2$Ru](PF_6)$_2$} contain the supplementary crystallographic data for this paper. These data can be obtained free of charge from The Cambridge Crystallographic Data Centre via www.ccdc.cam.ac.uk/data_request/cif.

Acknowledgments

This work was supported by the Deutsche Forschungsgemeinschaft (SFB 623) and by the European Commission (Marie Curie Intra-European Fellowship for H. S.).

[1] a) J. P. Collman, R. R. Gagné, C. A. Reed, *J. Am. Chem. Soc.* **1974**, *96*, 2629–2630; b) N. Kitajima, K. Fujisawa, C. Fujimoto, Y. Morooka, S. Hashimoto, T. Kitagawa, K. Toriumi, K. Tatsumi, A. Nakamura, *J. Am. Chem. Soc.* **1992**, *114*, 1277–1291.
[2] B. Kersting, *Z. Anorg. Allg. Chem.* **2004**, *630*, 765–780 and references cited therein.
[3] N. Le Poul, M. Campion, B. Douziech, Y. Rondelez, L. Le Clainche, O. Reinaud, Y. Le Mest, J. Am. Chem. Soc. **2007**, *129*, 8801–8810 and references cited therein.
[4] a) H. Vahrenkamp, *Acc. Chem. Res.* **1999**, *32*, 589–596; b) L. M. Mirica, X. Ottenwaelder, T. D. P. Stack, *Chem. Rev.* **2004**, *104*, 1013–1046.
[5] L. Kovbasyuk, R. Krämer, *Chem. Rev.* **2004**, *104*, 3161–3187.
[6] B. H. Peek, G. T. Ross, S. W. Edwards, G. J. Meyer, T. J. Meyer, B. W. Ericksson, *Int. J. Peptide Protein Res.* **1991**, *38*, 114–123.
[7] X. Li, C. L. D. Gibb, M. E. Kuebel, B. C. Gibb, *Tetrahedron* **2001**, *57*, 1175–1182.
[8] J. Gong, B. C. Gibb, *Org. Lett.* **2004**, *6*, 1353.
[9] W. Yang, H. Schmider, Q. Wu, Y.-Sh. Zhang, S. Wang, *Inorg. Chem.* **2000**, *39*, 2397–2404.
[10] W. R. McWhinnie, G. C. Kulasingam, J. C. Draper, *J. Chem. Soc.* **1966**, 1199–1203.
[11] a) L. J. Childs, M. Pascu, A. J. Clarke, N. W. Alcock, M. J. Hannon, *Chem. Eur. J.* **2004**, *10*, 4291–4300; b) E. S. Zvargulis, I. E. Buis, T. W. Hambley, *Polyhedron* **1995**, *14*, 2267–2273; c) R. K. Boggess, A. H. Lamson, S. York, *Polyhedron* **1991**, *10*, 2791–2798.
[12] R. T. Jonas, T. D. P. Stack, *Inorg. Chem.* **1998**, *37*, 6615–6629.
[13] P. L. Dedert, T. Sorrell, T. J. Marks, J. A. Ibers, *Inorg. Chem.* **1982**, *21*, 3506–3517.
[14] P. L. Dedert, J. S. Thompson, J. A. Ibers, T. J. Marks, *Inorg. Chem.* **1982**, *21*, 969–977.
[15] P. A. Anderson, F. R. Keene, J. M. Gulbis, E. R. T. Tiekink, *Z. Kristallogr.* **1993**, *206*, 275.
[16] D. Boys, C. Escobar, W. Zamudio, *Acta Crystallogr., Sect. C: Cryst. Struct. Commun.* **1992**, *48*, 1118.
[17] F. R. Keene, M. R. Snow, P. J. Stephenson, E. R. T. Tiekink, *Inorg. Chem.* **1988**, *27*, 2040–2045.
[18] N. Nagao, *Meiji Daigaku Kagaku Gijutsu Kenkyusho Nenpo* **1999**, *41*, 59.
[19] H. Irving, D. H. Mellor, *J. Chem. Soc.* **1962**, 5222–5237.
[20] a) T. Nabeshima, Y. Tanaka, T. Saiki, S. Akine, C. Ikeda, S. Sato, *Tetrahedron Lett.* **2006**, *47*, 3541–3544; b) E. Krenske, L. R. Gahan, *Aust. J. Chem.* **2002**, *55*, 761–766; c) L. Zelikovich, J. Libman, A. Shanzer, *Nature* **1995**, *374*, 790–792. A redox-dependent translocation of a single Fe ion between the two sites was also observed.
[21] M. Kodera, Y. Tachi, T. Kita, H. Kobushi, Y. Sumi, K. Kano, M. Shiro, M. Koikawa, T. Tokii, M. Ohba, H. Okawa, *Inorg. Chem.* **2000**, *39*, 226–234.
[22] G. A. Crosby, W. G. Perkins, D. M. Klassen, *J. Chem. Phys.* **1965**, *43*, 1498–1503.
[23] T. Bora, M. M. Singh, *J. Inorg. Nucl. Chem.* **1976**, *38*, 1815–1820.
[24] G. M. Sheldrick, *SADABS*, Bruker AXS, **2004**–**2008**.
[25] a) P. T. Beurskens in *Crystallographic Computing 3* (Eds.: G. M. Sheldrick, C. Krüger, R. Goddard), Clarendon Press, Oxford, UK, **1985**, p. 216; b) P. T. Beurskens, G. Beurskens, R. de Gelder, J. M. M. Smits, S. Garcia-Granda, R. O. Gould,

DIRDIF-2008, Raboud University Nijmegen, The Netherlands, **2008**.
[26] a) G. M. Sheldrick, *SHELXS-86*, University of Göttingen, **1986**; b) G. M. Sheldrick, *Acta Crystallogr., Sect. A* **1990**, *46*, 467.
[27] G. M. Sheldrick, *SHELXL-97*, University of Göttingen, **1997**; G. M. Sheldrick, *Acta Crystallogr., Sect. A* **2008**, *64*, 112.
Received: October 17, 2008
Published Online: December 2, 2008

